2022

New Results at JLab Describing Operating Lifetime of GaAs Photo-Guns

M. Bruker

J. Grames

C. Hernández-García

M. Poelker

S. Zhang

See next page for additional authors

Original Publication Citation

Bruker, M., Grames, J., Hernández-García, C., Poelker, M., Zhang, S., Lizárraga-Rubio, V., Valerio-Lizárraga, C., & Yoskowitz, J. T. (2022). New results at JLab describing operating lifetime of GaAs photo-guns. In S. Biedron, E. Simakov, S. Milton, P.M. Anisimov, & V.R.W. Schaa (Eds.) *Proceedings of the North American Particle Accelerator Conference* (pp.644-647). JACOW. https://doi.org/10.18429/JACoW-NAPAC2022-WEPA13

ISBN: 978-3-95450-232-5 ISSN: 2673-7000 doi:10.18429/JACoW-NAPAC2022-WEPA13

NEW RESULTS AT JLAB DESCRIBING OPERATING LIFETIME OF GaAs PHOTO-GUNS*

M. Bruker†, J. Grames, C. Hernández-García, M. Poelker, S. Zhang
Thomas Jefferson National Accelerator Facility, Newport News, VA, USA
V. Lizárraga-Rubio, C. Valerio-Lizárraga, FCFM-UAS, Culiacan, Sinaloa, Mexico
J. T. Yoskowitz, Old Dominion University, Norfolk, VA, USA

Abstract

Polarized electrons from GaAs photocathodes have been key to some of the highest-impact results of the Jefferson Lab science program over the past 30 years. During this time, various studies have given insight into improving the operational lifetime of these photocathodes in DC high-voltage photo-guns while using lasers with spatial Gaussian profiles of typically 0.5 mm to 1 mm FWHM, cathode voltages of 100 kV to 130 kV, and a wide range of beam currents up to multiple mA. In this contribution, we show recent experimental data from a 100 kV to 180 kV setup and describe our progress at predicting the lifetime based on the calculable dynamics of ionized gas molecules inside the gun. These new experimental studies at Jefferson Lab are specifically aimed at exploring the ion damage of higher-voltage guns being built for injectors.

INTRODUCTION

Polarized photoelectron guns employ a photocathode with a certain chemical composition and surface structure designed to absorb photons and photoemit free electrons. The constant of proportionality between the two, η, is called *quantum efficiency* (QE):

$$\eta = \frac{\text{number of electrons}}{\text{number of photons}} = \frac{I}{P}\frac{hc}{e\lambda} \tag{1}$$

with the electron current I, the laser power P, and the laser wavelength λ.

Photocathodes are subject to various damage mechanisms that reduce η as a function of time or extracted charge; GaAs, while important because of the high degree of spin polarization it provides [1], is a particularly sensitive cathode material. Despite technological advances that have had dramatic effects in reducing damage rates – e.g., improving gun vacuum, suppressing beam loss originating from stray light, or reducing laser heating – the prevailing limitation remains: ionized residual-gas molecules being accelerated backwards by the electric field in the gun acceleration gap and colliding with the cathode surface, which is referred to as *ion back-bombardment* [2–4].

Because these ions are generated by the electron beam, their total number scales with extracted charge. Although the physical mechanism by which they degrade the QE is still subject to research [5], the decay rate is observed to be characteristically exponential, giving rise to the concept of a *charge lifetime* τ_C, i.e.,

$$\eta(Q) = \eta_0 \exp\left(Q/\tau_C\right) \tag{2}$$

for any integrated amount of charge Q.

In recent years, there has been considerable development to increase the maximum voltage of DC photo-guns, primarily to reduce space-charge effects in the beam [6], but also with the expectation that the rate of ion back-bombardment should fall. Figure 1(top) shows that the ionization cross section for H_2, the predominant gas in a baked photogun, declines logarithmically with electron energy. Taking into account the field geometry of the cathode-anode gap, while the maximum ion production takes place just in front of the photocathode, there are still substantial contributions from high-energy ions, see Fig. 1(bottom). As ion energy factors into photocathode damage vis-a-vis the roles of ion sputtering and ion implantation [5], lifetime improving with higher voltage is not necessarily a given.

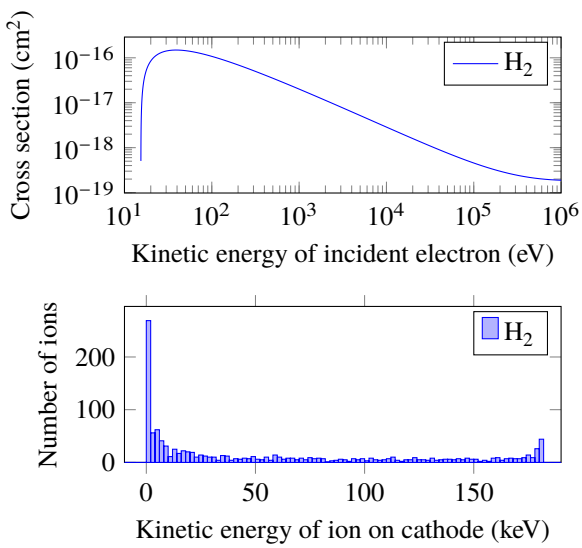

Figure 1: Ionization cross section of H_2 [7, 8] (top) and histogram of simulated kinetic energies of ions for a real gun geometry at 180 kV gun voltage (bottom). This simulation was performed with GPT as described below and assumes a homogeneous molecule density of 3×10^{10} m^{-3} and an extracted charge of 1 mC; the cathode-anode distance is 8 cm. The number of ions scales with gas density and charge.

* This material is based upon work supported by the U.S. Department of Energy, Office of Science, Office of Nuclear Physics under contract DE-AC05-06OR23177.
† bruker@jlab.org

ISBN: 978-3-95450-232-5 ISSN: 2673-7000 doi:10.18429/JACoW-NAPAC2022-WEPA13

EXPERIMENTAL SETUP AND DATA

Aiming to determine the dependency between gun voltage and cathode lifetime, we performed an exploratory experiment at the Upgraded Injector Test Facility (UITF) at Jefferson Lab, which features an inverted-insulator photo-gun similar to the one installed at CEBAF [9]. In this experiment, a constant-current electron beam was extracted from the gun and transported to a dump while observing the QE over a period of time sufficient to measure degradation. Generally, all beam parameters were kept constant, the current being controlled by a software feedback loop as illustrated in Fig. 2. The dump is located behind a series of apertures with individual vacuum pumps for each segment, providing good gun vacuum isolation from downstream beam-current-dependent gas loads.

As a main challenge of this experiment lies in keeping parameters as similar as possible for weeks in the face of practical conditions, such as turning off and on again over night, accessing the vault, etc., it is desirable to choose the maximum value of beam current that can be sustained throughout the studies despite QE degradation. In the present setup, the available beam current is mostly determined by the laser system, which includes an optical fiber that limits the power at the cathode to about 50 mW. The beam current chosen for the experiment was initially 500 µA and was later reduced to 300 µA.

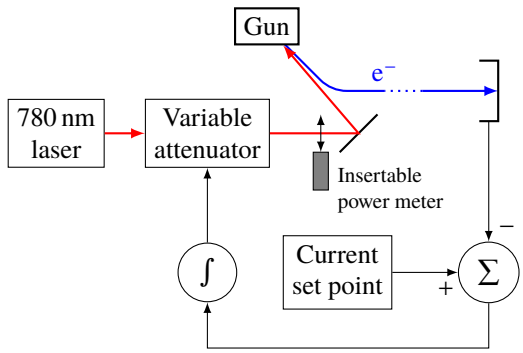

Figure 2: Simplified schematic of the beam-current lock at the UITF.

The gun anode is biased to +2.5 kV throughout the whole study[1], creating a potential barrier that repels all ions generated downstream [4, 11].

The QE distribution of the photocathode is measured between runs, but this takes 40 min and therefore cannot be done parasitically during the runs. To obtain lifetime data with any time resolution, we periodically insert the laser power meter during beam runs; as the electron beam current is constant and known, η follows from Eq. 1. We then extract τ by windowing the η data; the result of our first study is shown in Fig. 3. The data suggest that lifetime at 100 kV tends to be higher than at 180 kV; however, the dependency is obfuscated by an overall increase in lifetime, warranting a systematic study to understand the behavior. The following sections describe mechanisms we believe are important to interpreting this result and improving future studies.

[1] While the initial energy distribution of the ions is assumed to be mostly thermal, the applied voltage also accounts for both the residual on-axis cathode-anode field and any additional beam potential that would subtract from it [10].

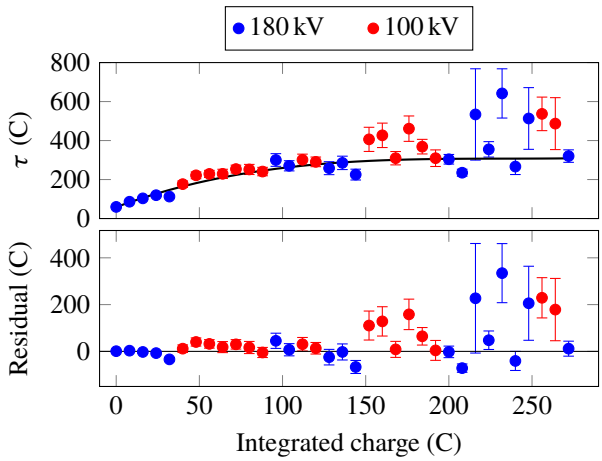

Figure 3: Evolution of lifetime throughout the experiment, windowed over a charge of 8 C. As the voltage dependency is masked by an overall increase whose functional dependency is, a priori, unknown, we use an error-weighted smoothing spline (solid black line) to get a sense of the residuals.

EFFECT OF LASER SPOT SIZE ON LIFETIME

Simulations of ion generation and trajectories were performed using the particle tracking code GPT [12] with an electrostatic model of the gun and a custom element to simulate electron-impact ionization of residual gas [13] using the cross-section data from [7]. As a first study, we simulated the effect of laser position and size: as the spot size increases, so does the size of the damage area on the photocathode, reducing the damage density. With this, the QE lifetime is expected to improve, as has been shown experimentally at CEBAF [4, 14]. The 2D ion profiles for two simulations with different laser spot sizes are shown in Fig. 4. As space charge is neglected, the model scales with gas density and extracted charge; throughout this study, we universally assume a molecule density of 3×10^{10} m^{-3} and an extracted charge of 1 mC. The numbers are then scaled as needed.

ITERATIVE MODEL FOR QE DEGRADATION

Because the electron beam profile is the product of the QE distribution and the laser profile, the RMS size of the electron beam generally becomes larger than that of the laser spot as the QE is locally degraded. Figure 5 illustrates this concept.

We created a simulation model based on this idea that starts with a homogeneous QE distribution on a discrete grid, a realistic laser spot size of $\sigma_x = \sigma_y = 0.4$ mm, and an

ISBN: 978-3-95450-232-5 ISSN: 2673-7000 doi:10.18429/JACoW-NAPAC2022-WEPA13

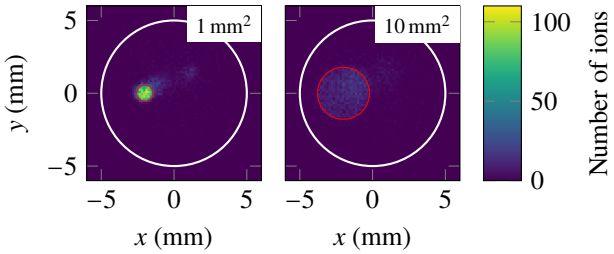

Figure 4: Example ion distributions for laser spot sizes of 1 mm² and 10 mm², respectively. In these simulations, the laser spot is displaced horizontally by −2 mm as denoted by the red circle. The white circle represents the active area with a radius of 5 mm.

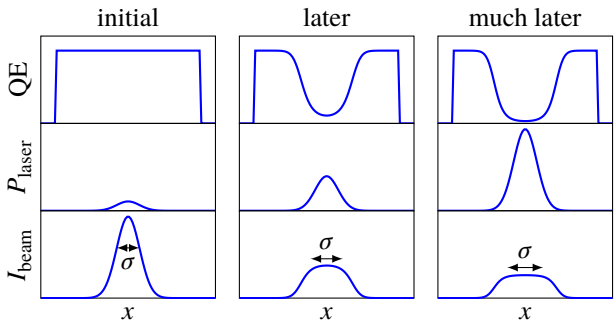

Figure 5: Simplified model assuming QE degradation is proportional to electron emission at any position. Localized degradation results in beam being emitted predominantly by the tails of the laser spot, giving a flat-top beam with higher RMS width over time.

assumption for a *damage function*, i.e., the damage caused by each ion as a function of energy; this function is the only degree of freedom as the kinematics of both electrons and ions can be calculated from first principles, using the same electrostatic model and GPT module as in the previous section. The total number of particles is kept constant, corresponding to constant current. Applying the resulting damage to the QE distribution, we can iterate with arbitrary granularity. The process is shown schematically in Fig. 6.

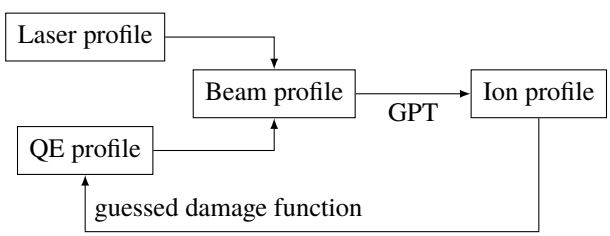

Figure 6: Principle of simulating QE degradation.

As a first test, we choose the damage function as

$$F = \exp\left(-\alpha E_{\mathrm{kin}}\right) \tag{3}$$

with E_{kin} being the total kinetic energy of the ions deposited in one grid tile and $\alpha = 5 \times 10^{-7}\ \mathrm{eV}^{-1}$ as an educated guess. The evolution of the lifetime is shown in Fig. 7.

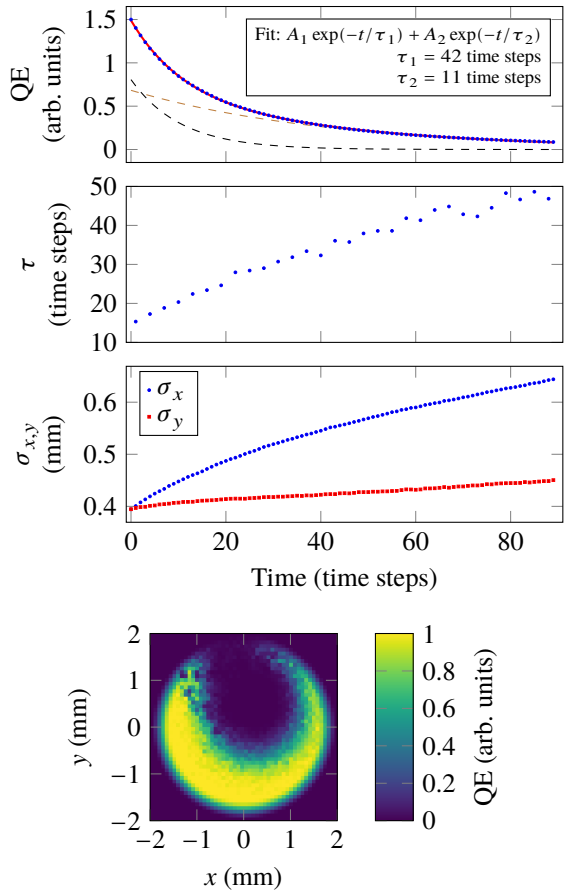

Figure 7: Simulated QE evolution at the laser spot position. The double-exponential behavior is qualitatively similar to what was observed in the experiment (dashed lines show the exponentials individually). The beam profile gets widened more strongly in x than in y because the field geometry of the gun displaces high-energy ions vertically, preventing them from damaging the emitting area. The bottom figure shows the QE distribution after the last time step.

Apart from the one-dimensional data set of lifetime vs. charge, this iteration yields the whole QE distribution as a function of integrated charge that can be compared with experimental data. Even though the measured QE degradation is a convolution of the true distribution with the laser profile and cannot be deconvolved, this model approach allows us to dynamically simulate ion damage for comparison to model damage mechanisms and extract physical model parameters.

CONCLUSION

Fully understanding photocathode ion damage requires a model that predicts both the ion distribution on the cathode and the resulting impact on the QE. Computing the former from first principles may allow us to determine the latter by comparison with experimental data. However, this relies on reproducible experimental conditions, e.g., same extracted charge per run; improving the setup is therefore a necessary next step.

ISBN: 978-3-95450-232-5 ISSN: 2673-7000 doi:10.18429/JACoW-NAPAC2022-WEPA13

REFERENCES

[1] T. Maruyama *et al.*, "A very high charge, high polarization gradient-doped strained GaAs photocathode," *Nucl. Instrum. Methods Phys. Res., Sect. A*, vol. 492, pp. 199–211, 2002. doi:10.1016/S0168-9002(02)01290-1

[2] K. Aulenbacher *et al.*, "Operating experience with the MAMI polarized electron source," in *Proc. Workshop on Photocathodes for Polarized Electron Sources for Accelerators*, SLAC, Stanford, CA, 1994, pp. 1–12.

[3] J. Grames *et al.*, "Ion Back-Bombardment of GaAs Photocathodes Inside DC High Voltage Electron Guns," in *Proc. PAC'05*, Knoxville, TN, USA, May 2005, pp. 2875–2877. https://jacow.org/p05/papers/WPAP045.pdf

[4] J. Grames *et al.*, "Charge and fluence lifetime measurements of a dc high voltage GaAs photogun at high average current," *Phys. Rev. ST Accel. Beams*, vol. 14, p. 043 501, 2011. doi:10.1103/PhysRevSTAB.14.043501

[5] W. Liu, S. Zhang, M. Stutzman, and M. Poelker, "Effects of ion bombardment on bulk GaAs photocathodes with different surface-cleavage planes," *Phys. Rev. Accel. Beams*, vol. 19, p. 103 402, 2016. doi:10.1103/PhysRevAccelBeams.19.103402

[6] R. Kazimi, A. Freyberger, F. E. Hannon, A. S. Hofler, and A. Hutton, "Upgrading the CEBAF Injector with a New Booster, Higher Voltage Gun, and Higher Final Energy," in *Proc. IPAC'12*, New Orleans, LA, USA, May 2012, pp. 1945–1947. https://jacow.org/IPAC2012/papers/TUPPR055.pdf

[7] M. Reiser, *Theory and Design of Charged Particle Beams*. John Wiley & Sons, Ltd, 2008. doi:10.1002/9783527622047

[8] L. J. Kieffer and G. H. Dunn, "Electron Impact Ionization Cross-Section Data for Atoms, Atomic Ions, and Diatomic Molecules: I. Experimental Data," *Rev. Mod. Phys.*, vol. 38, pp. 1–35, 1 1966. doi:10.1103/RevModPhys.38.1

[9] J. M. Grames *et al.*, "CEBAF 200 kV Inverted Electron Gun," in *Proc. PAC'11*, New York, NY, USA, Mar.-Apr. 2011, pp. 1501–1503. https://jacow.org/PAC2011/papers/WEODS3.pdf

[10] J. Grames *et al.*, "A Biased Anode to Suppress Ion Back-Bombardment in a DC High Voltage Photoelectron Gun," *AIP Conference Proceedings*, vol. 980, pp. 110–117, 2008. doi:10.1063/1.2888075

[11] J. T. Yoskowitz *et al.*, "Improving the Operational Lifetime of the CEBAF Photo-Gun by Anode Biasing," in *Proc. IPAC'21*, Campinas, Brazil, May 2021, pp. 2840–2842. doi:10.18429/JACoW-IPAC2021-WEPAB104

[12] Pulsar Physics. "General Particle Tracer." (2022), http://www.pulsar.nl/gpt

[13] J. T. Yoskowitz, J. M. Grames, G. A. Krafft, G. R. M. Soto, C. A. Valerio, and S. B. van der Geer, "Simulating Electron Impact Ionization Using a General Particle Tracer (GPT) Custom Element," in *Proc. IPAC'21*, Campinas, Brazil, May 2021, pp. 2843–2846. doi:10.18429/JACoW-IPAC2021-WEPAB105

[14] J. Grames *et al.*, "Milliampere beam studies using high polarization photocathodes at the cebaf photoinjector," *Proc. XVII International Workshop on Polarized Sources, Targets & Polarimetry — PoS(PSTP2017)*, vol. 324, p. 014, 2018. doi:10.22323/1.324.0014